



HAL
open science

Coulomb stress evolution along the Kongur Extensional System since 1895 and present seismic hazard

Wei Xiong, Xuejun Qiao, Gang Liu, Wei Chen, Zhaosheng Nie

► **To cite this version:**

Wei Xiong, Xuejun Qiao, Gang Liu, Wei Chen, Zhaosheng Nie. Coulomb stress evolution along the Kongur Extensional System since 1895 and present seismic hazard. *Geodesy and Geodynamics*, 2019, 10, pp.1 - 9. <10.1016/j.geog.2018.11.007>. <hal-03487041>

HAL Id: hal-03487041

<https://hal.science/hal-03487041v1>

Submitted on 20 Dec 2021

HAL is a multi-disciplinary open access archive for the deposit and dissemination of scientific research documents, whether they are published or not. The documents may come from teaching and research institutions in France or abroad, or from public or private research centers.

L'archive ouverte pluridisciplinaire HAL, est destinée au dépôt et à la diffusion de documents scientifiques de niveau recherche, publiés ou non, émanant des établissements d'enseignement et de recherche français ou étrangers, des laboratoires publics ou privés.



Distributed under a Creative Commons CC BY-NC 4.0 - Attribution - Non-commercial use - International License

Coulomb Stress Evolution along the Kongur Extensional System Since 1895 and Present Seismic Hazard

Wei Xiong^{a,b}, Xuejun Qiao^{a*}, Gang Liu^a, Wei Chen^a, Zhaosheng Nie^a

^a Key Laboratory of Earthquake Geodesy, Institute of Seismology, China Earthquake Administration, Wuhan 430071, China

^b School of Geodesy and Geomatics, Wuhan University, Wuhan 430079, China

* Corresponding author.

E-mail addresses: xiongwei_19881229@163.com (Wei Xiong); xuejunq@sohu.com (XuejunQiao).

Abstract: The present-day tectonic activities on the northeastern margin of the Pamir Plateau are mainly E-W oriented extensions, among which the Kongur Extensional System (KES) plays an important role in the internal expansion of the Pamir. As the largest earthquake since Taxkorgan earthquakes in 1895 and 1896, the Aketao earthquake occurred on the Muji fault on the northern portion of the KES in 2016. Since then, the trend of seismic activities along the KES has been paid much attention to. Based on the viscoelastic layered lithosphere model, we calculate the co-seismic and post-seismic stress changes caused by five historical earthquakes on the KES and its adjacent areas since 1895, and analyze the interaction among strong earthquakes. The results show that all of the historical earthquakes after 1895 occurred in the areas where the co-seismic and post-seismic Coulomb stress increased. Coulomb stress loading at the hypocenters of the 1896 Taxkorgan earthquake, the 1974 Markansu earthquake and the 2016 Aketao earthquake were 0.251 MPa, 0.013 MPa and 0.563 MPa, respectively. The three earthquakes were catalyzed by such variations. The historical earthquakes increased the stress state on most segments of the Southern Kungai Mountain fault and Kongur fault along the KES. In particular, we can identify 2 visible earthquake gaps with increasing seismic hazard formed on the Qimugan segment and Bulunkou segment of the KES. The Qimugan section and the Bulunkou section are located at the fault transition zone with concentrated stress and high extension rate, so great attention should be paid to their seismic hazard at present day.

Key words: Kongur extensional system;Coulomb stress; stress accumulation; seismic hazard

1 Introduction

In the past 50 to 55 million years, the Indian Plate thrust underneath the Eurasian Plate at a relative speed of 40 ~ 50mm/a, causing extensive deformation within the Eurasian continent. Mountains in the Pamir region were greatly uplifted, with widely developed faults and frequent earthquakes[1]. Since the Late Cenozoic, the northeastern Pamir has experienced large regional tectonic deformation characterized by the shortening, strike slip and internal extension. A series of active tectonic zones (Fig. 1) hence came into being, including the Kongur Extensional System (KES), the Main Pamir Thrust (MPT), the Pamir Frontal Thrust (PFT), and the Markansu Fault[2].At present, the active deformation in the northeastern Pamir is mainly concentrated on the KES, the PFT and the Artux-Kash folded belt, and these active faults control the occurrence of strong earthquakes ($M_w > 7.0$) in the northeastern Pamir[3].

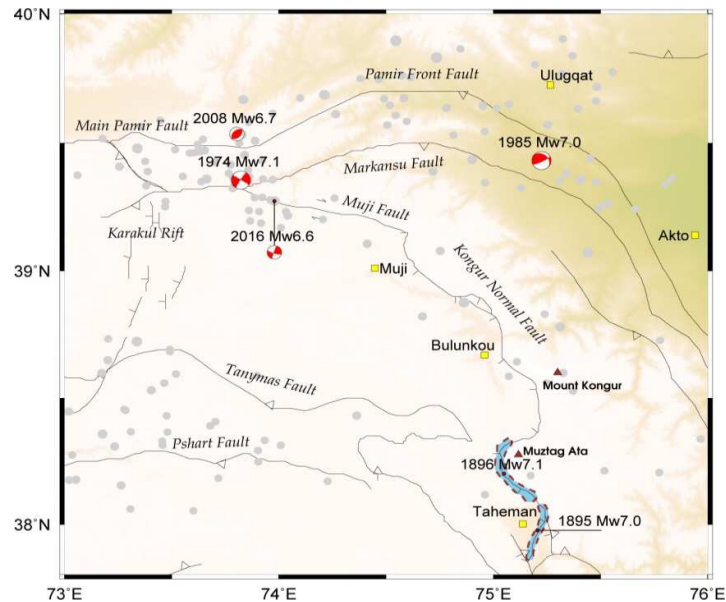


Fig. 1: Main faults and historical earthquakes along the KES and its surroundings. (The black lines represent the main active faults marked with names of the faults in the study zone; the red focal spheres represent the locations of historical seismicity and the focal mechanisms; the area surrounded by the dotted line represents the rupture zone of two historical earthquakes in 1895 and 1896[3]; the gray dots represent the mid-size earthquakes between 1895 and 2017;and the yellow squares represent the main cities in the study area.)

On November 25, 2016 at 22:24 pm, an $M_w6.6$ earthquake happened in Aketao County, Xinjiang Uygur Autonomous Region. The epicenter was located at 39.238° N , 74.047° E , and the focal depth was $12.6 \pm 3 \text{ km}$ (United States Geological Survey, USGS). The Aketao earthquake which occurred on the Muji fault is the largest earthquake on the KES since the 1895 and 1896 Taxkorgan earthquakes. The relationship between the Aketao earthquake and the historical events and the future trend of seismic activities along the KES have become urgent concerns [4]. It is worth noting that two $M_w 6.0$ earthquakes (Fig. 1) occurred on November 3, 2008 and June 26, 2016 at the Sino-Kyrgyz border. In addition, on December 7, 2015, an $M_w7.2$ earthquake happened in Murghob, Tajikistan on the Karakul Rift, about 160 km southwest of the Aketao earthquake [5]. It may indicate that seismicity in the northeastern Pamir is becoming increasingly active [4]. After the Aketao earthquake, the trend of seismic activities in the northeastern Pamir, especially in the KES and its surrounding areas has received much attention. However, due to the poor geographical conditions in the northeastern Pamir, little geodetic data are available, and few studies have been made on the seismic hazard in this area.

Since the KES is one of the most seismically active faults in northeastern Pamir, the spatial and temporal dependent distribution of strong earthquakes and their interaction are important for assessing seismic hazard on the KES and surrounding areas. Adjacent strong earthquakes tend to impact and interact with each other. Such interaction can be quantitatively described through Coulomb stress change caused by co-seismic and post-seismic deformation, which further provides a reference for determining seismic hazard in active fault zones [6]. If an earthquake causes stress loading on a receiver fault, it may bring the fault closer to rupture; contrarily, if an earthquake causes negative Coulomb Stress change on a receiver fault, it may retard subsequent events [7-9]. Based on the co-seismic and post-seismic Coulomb stress changes caused by historical strong earthquakes, many studies have successfully acquired the stress variation of active faults and evaluated their seismic risk. Parsons et al. [10] calculated the effect of the 1999 Izmit earthquake on the faults near Istanbul, suggesting that the earthquake increased the occurrence probability of strong earthquakes in Istanbul over the next 30 years. Xiong et al. [11] studied the stress evolution caused by historical strong earthquakes along Kunlun Fault, and found that all these historical earthquakes occurred in the positive stress zone caused by the preceding earthquakes. Based on the co-seismic and post-seismic viscoelastic stress change and inter-seismic

stress accumulation, Shan et al.[12]obtained the characteristics of Coulomb stress evolution along the Xianshuihe-Xiaojiang fault since 1713, and concluded that the seismic activity in four seismic gaps was increased. The theory of Coulomb stress change provides us an important tool to assess time-dependent earthquake hazard.

In this work, we collected a sequence of 5 $M_w > 7$ earthquakes (Table 2 and Fig.1) that occurred on the KES and its surrounding areas since 1895. Based on the co-seismic and post-seismic stress disturbances caused by historical earthquakes, we obtain the characteristics of stress evolution along the KES, and identify the stress accumulation in present days. We then analyze the interaction among historical earthquakes and the future seismic trend in fault zones, and provide a reference for seismic hazard assessment in the study area.

2. Neotectonics and historical seismicity

2.1 Kinematic characteristics of the KES

According to the geometric characteristics, present terrain and lithological features of faults, the KES can be divided into five sections from the north to the south: the Mujidextral strike slip fault, the northern segment of Kungai Mountain normal fault, the southern segment of Kungai Mountain normal fault, the Kongur normal fault, and Muztag normal fault [2] (Fig. 1, Table 1). The KES can also be divided into two segments –the southern and northern segments at Muztag Mountain. The present tectonic movement along the whole KES is not uniform, as the E-W oriented extension rate is decreasing from the south to the north: the right lateral rate on Muji fault, the northernmost part of the KES, is 4.5-11mm/a [13], while the extension rate on the Muztag fault, the southern part of the KES, is less than 2mm/a. In addition, there are the Taheman and the Taxkorgan normal fault on the south of the Muztag normal fault, and the E-W extension rate of the Taxkorgan normal fault is less than 1 mm/a [3].

As a huge tectonic obstacle, the Muztag Mountain divided the KES into the southern and northern segments, making seismic activities on these two segments independent from each other. However, the Muji Fault, the Kungai Normal Fault, the Kongur Normal Fault and the Muztag Normal Fault are all capable of generating $M_w > 7.0$ earthquakes independently. According to the field investigation along these faults, the magnitudes of the paleo-earthquakes were $M_w 7.0-7.5$ [3].

Table 1 Kinematic parameters of different sections along the KES [2-3,13]

Fault	Dislocation mechanism	Orientation	Dip (°)	Rake (°)	E-W extension rate (mm/a)	Strike-slip rate/dip-slip rate (mm/a)
Muji Fault	Strike-slip/Normal	Southwest	75~90	-160~-1 80	4.5~11	4.5~11
Northern Segment of Kungai Fault	Normal	West	~20	-90	~6.8	~7.2
Southern Segment of Kungai Fault	Normal	West	30~45	-90	~6.8	~8.8
Kongur Fault	Normal	West	~40	-90	~5.4	~6.5
Muztag Fault	Normal	West	~40	-90	~3	~3.9

2.2 Hypocenter parameters of historical earthquakes

On July 5, 1895, an $M_w7.0$ earthquake struck Taxkorgan in the southern segment of the KES, brought the southern segment of the Muztag Fault and the whole Taheman Fault to rupture, and generated a 27km long fracture zone. Following the $M_w7.0$ Taxkorgan earthquake, an $M_w7.1$ earthquake occurred at the west side of Muztag Mountain on March 4, 1896, which led to rupture at the middle part of the Muztag Fault and generated a 20-km-long fracture zone. These two are the most severe normal fault earthquakes that occurred in the northeastern Pamir in recent 120 years, and also the largest earthquakes on the southern segment of the KES that have been thoroughly studied before [2-3]. Li et al. [3] conducted two large-scale field geological mappings and differential GPS measurements on the coseismic rupture zones of these two earthquakes, and obtained their hypocenter parameters and slip distribution models (Fig. 1).

On August 11, 1974, Markansu $M_w7.1$ earthquake shook the north of the western Markansu Fault, and no surface rupture was found in the epicenter [14]. Based on the P-wave and S-wave initial motion, Jackson et al. [15] obtained the focal mechanism of this earthquake (Fig. 1, Table 2). They considered that the earthquake was dominantly dextral strike slip, which is consistent with the conclusion made by Yang et al. [16]. In addition, the aftershock sequence relocations show that the aftershocks are mainly distributed along an N-W band with a width of 20 km and a length of 45 km, which also sketches the maximum range of the main shock slip [15].

On August 23, 1985, Ulugqat $M_w 7.0$ earthquake occurred on Mingyaoler anticline and caused a 15-km-long rupture zone [17]. The rupture is quite complex and hard to be fitted by point source model. Burtman et al.[18] provided the focal mechanism solution of this earthquake and concluded that the main shock might consist of three subevents, namely one thrust fault and two right-lateral thrust faults (Fig. 1, Table 2).

The results of several calculations show that the ranges and magnitudes of stress disturbances caused by $M_w < 6.5$ earthquakes along the KES and $M_w < 7$ earthquakes in surrounding areas are relatively small (for example, the $M_w 6.7$ Ulugqat earthquake in 2008 only caused slight stress change, amounting to KPa at the hypocenter of Aketao earthquake), which cannot exert a significant effect on the stress state of the KES. Therefore, we do not take these historical earthquakes into account. We selected the above four earthquakes in the study area with clear focal mechanism or slip model and the 2016 Aketao earthquake as historical seismic events (Table 2). The slip models of the 1895 Taxkorgan, 1896 Taxkorgan and 2016 Aketao earthquakes are obtained from references, and the rupture parameters (rupture length, rupture width, slip) of the other historical earthquakes are calculated based on empirical equations[19]. Similar methods are widely used in studies on the stress evolution along active faults [12, 20-21].

Table 2 Model parameters of historical earthquakes [3, 15-18, 22]

Time	Magnitude	Epicenter location		Focal mechanism			Focal depth	Focal distribution		
		Longitude (°E)	Latitude (°N)	Strike (°)	Dip (°)	Rake (°)	km	Length (km)	Width (km)	Slip (m)
1895	$M_w 7.0$	75.236	38.000	-	-	-	15	-	-	-
1896	$M_w 7.1$	75.05	38.20	-	-	-	15	-	-	-
1974	$M_w 7.1$	73.806	39.381	302.6	87.6	173.6	23	67.9	14.4	1.2
1985	$M_w 6.3$			283	34	142	18	17.4	9.5	0.4
(3 sub	$M_w 6.5$			326	58	158	19	23.6	11.8	0.5
events)	$M_w 6.6$			309	41	152	18	25.7	12.5	0.6
2016	$M_w 6.6$	74.04	39.27	303	74	-162	10	-	-	-

3. Models and Methods

3.1 Model for Coulomb failure stress

When an earthquake occurs, there are relatively large static co-seismic slips that trigger static co-seismic strain and stress on the causative fault. Since the lower crust and the upper mantle are viscoelastic, strain is slowly released, gradually causes post-seismic surface displacement, and consequently produces viscoelastic relaxed strain and stress that change with time. Both co-seismic and post-seismic stress adjustments can cause Coulomb stress changes on a receiver fault. According to the Coulomb failure law, the Coulomb stress change on a receiver fault is:

$$\Delta\sigma_f = \Delta\tau + \mu(\Delta\sigma_n + \Delta P) \quad (1)$$

where $\Delta\tau$ is the shear stress change on the fault (positive - reckoned in the direction of fault slip), and $\Delta\sigma_n$ is the normal stress change (positive if the fault is unclamped). ΔP is the pore pressure change in the fault zone (positive in compression), and μ is the friction coefficient (with a range of 0~1). Rupture is encouraged if $\Delta\sigma_f$ is positive and restrained if negative; both the increased shear stress and unclamping of faults can promote failure. The tendency of ΔP counteracts that of $\Delta\sigma_n$. Hence, ΔP and $\Delta\sigma_n$ are merged into one term by introducing the “effective” friction coefficient μ' in equation (1) [23], composing the following equation:

$$\Delta\sigma_f = \Delta\tau + \mu'\Delta\sigma_n \quad (2)$$

Values for effective friction coefficient are often assigned based on experience, for it is almost impossible to actually measure and determine them on the receiver fault [24]. Parsons et al. [24] held that the effective friction coefficient of a high-angle strike-slip fault should be low, while that of a dip-slip fault should be high. In this paper, the effective friction coefficient is assumed to be 0.4 for calculation, and the effect of different coefficients on the ultimate result is discussed.

We use the PSCMP/PSGRN software[25] to calculate the co-seismic and post-seismic Coulomb stress change. Based on a layered viscoelastic half space model with gravity effects, this software can effectively simulate the Coulomb stress change caused by earthquakes.

3.2 Lithospheric stratification

Based on Crust 1.0, we obtain the parameters of stratified lithosphere in the study area. Poisson's ratio is assumed to be 0.25, and Linear Maxwell rheology is used to simulate the

rheological structure of the lower crust and upper mantle (Table 3). For the stress evolution of the Himalayan Main Frontal Thrust, Xiong et al. [21] set the viscosity coefficients of the lower crust and the upper mantle as $1 \times 10^{19} \text{Pa}\cdot\text{s}$ and $1 \times 10^{20} \text{Pa}\cdot\text{s}$, respectively. Shan et al. [12] and Shi et al. [26] adopted the same coefficient values. However, for the post-seismic deformation caused by the 2001 Kokoxili earthquake, Wen et al. [27] took $2 \times 10^{19} \text{Pa}\cdot\text{s}$ as the viscosity value; and Xiong et al. [11] adopted a lower-crust viscosity coefficient of $1 \times 10^{18} \text{Pa}\cdot\text{s}$ to analyze the interaction between strong earthquakes along the Kunlun Fault. In this work, the viscosity coefficients of the lower crust and the upper mantle are set as $1 \times 10^{19} \text{Pa}\cdot\text{s}$ and $1 \times 10^{20} \text{Pa}\cdot\text{s}$. Values of these coefficients will exert an effect on the rate of post-seismic Coulomb stress change. In the following, we will discuss the effect of different values on the ultimate results.

Table3 Stratified model comprised of elastic upper crust, viscoelastic lower crust and viscoelastic mantle in study area

Stratum	Depth(km)	P-wave velocity(km/s)	S-wave velocity(km/s)	Density (kg/m^3)	Viscosity coefficients($\text{Pa}\cdot\text{s}$)	
Crust	Upper crust	0~0.5	3.40	1.73	2290	0
		0.5~23.45	6.00	3.52	2720	0
	Lower crust	23.45~36.16	6.30	3.68	2790	1×10^{19}
		36.16~49.92	6.60	3.82	2850	
Upper mantle	49.92~150	8.16	4.53	3360	1×10^{20}	

Note: The viscosity coefficients of the lower crust and the upper mantle are set as $1 \times 10^{19} \text{Pa}\cdot\text{s}$ and $1 \times 10^{20} \text{Pa}\cdot\text{s}$ (model 1). The viscosity coefficient of the lower crust selected by model 2 ($1 \times 10^{18} \text{Pa}\cdot\text{s}$) and model 3 ($2 \times 10^{19} \text{Pa}\cdot\text{s}$) will be used in stability analysis.

4. Calculations and Analysis

4.1 Stress transfer and earthquake interaction on the KES

Positive Coulomb stress change brings the fault closer to failure and thus earthquake occurrence, while negative Coulomb stress change retards subsequent events [7]. Based on this hypothesis, we adopt PSGRN/PSCMP software [25] to calculate the co-seismic and post-seismic effects of historical earthquakes on subsequent earthquake on the KES, and analyze the interaction between these earthquakes. The mechanism of receiver fault selected in our calculation is the focal

mechanism of corresponding historical earthquakes.

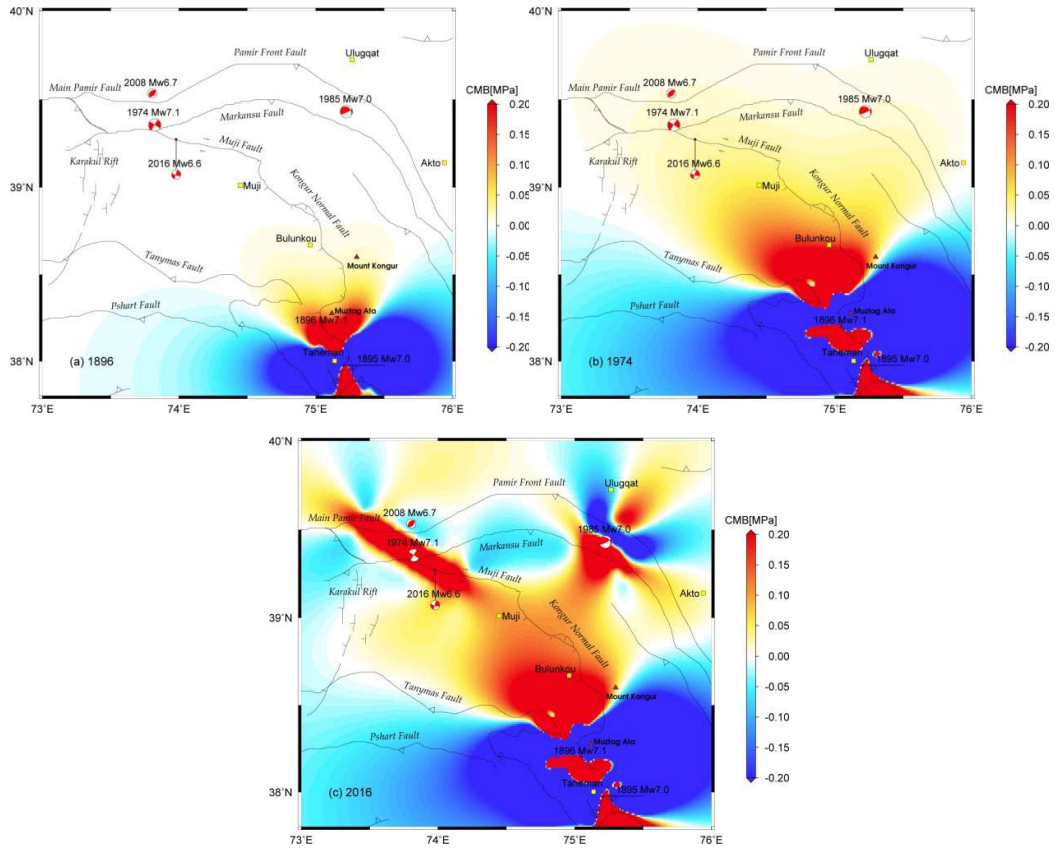


Fig.2 co-seismic and post-seismic Coulomb stress evolution caused by historical earthquakes since 1895

along the KES

- (a) Just before the 1896 earthquake;
- (b) Just before the 1974 earthquake;
- (c) Just before the 2016 earthquake

Calculations show that the 1895 earthquake caused significantly stress loading on the rupture plane of later 1896 earthquake, and the Coulomb stress change at the hypocenter was 0.251MPa (Fig.2a, Fig.3a). The average stress loading was greater than 0.1MPa, exceeding the threshold value of 0.01 MPa[7]. Therefore, the 1896 earthquake is significantly promoted by the co-seismic and post-seismic stress change caused by the 1895 earthquake.

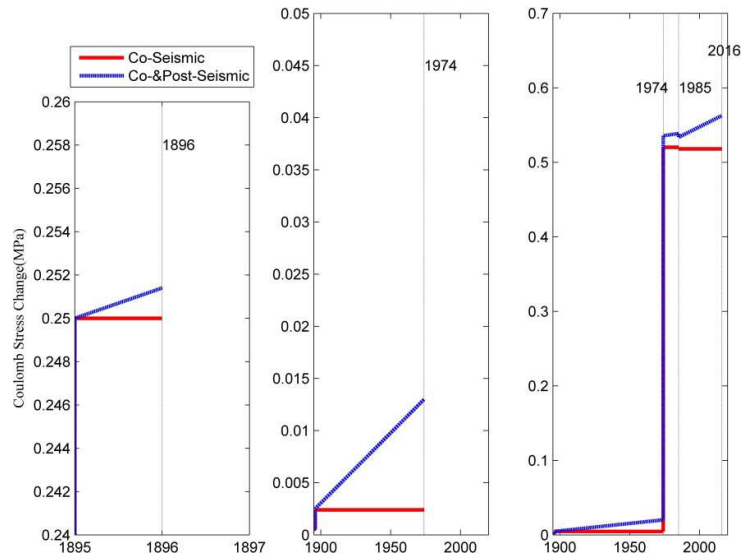


Fig. 3 Co-seismic and post-seismic stress evolution at the hypocenters of historical earthquakes along the KES since 1895

(a) before the 1896 earthquake; (b) before the 1974 earthquake; (c) before the 2016 earthquake

The 1974 earthquake occurred at the Uzbel Pass to the north of the western Markansu Fault, about 200 km away from the rupture plane of the 1895 and 1896 Taxkorgan earthquakes. Hence, after the 1896 earthquake, the variation of accumulated co-seismic Coulomb stress at the hypocenter of the 1974 earthquake was only 0.003MPa. However, due to the post-seismic viscoelastic relaxation of the lower crust and the upper mantle, the stress was gradually released and dispersed to far field. When the 1974 earthquake occurred, the Coulomb stress change at its hypocenter had come to 0.013 MPa (Fig. 2b, Fig. 3b), exceeding the threshold value 0.01 MPa for stress triggering. Therefore, the co-seismic and post-seismic process of historical earthquakes promoted the 1974 Markansu earthquake, and the post-seismic viscoelastic Coulomb stress change played an important role in the stress evolution of its adjacent region.

Since the 1895 and 1896 Taxkorgan earthquakes, the 2016 Aketao earthquake is the largest event along the KES. However, the hypocenters of the former two earthquakes are far from that of the latter one, so their co-seismic and post-seismic effects on the stress at the hypocenter of the Aketao earthquake are relatively slight. In addition, the 1985 Ulugqat earthquake generated a co-seismic Coulomb stress change of -0.002MPa at the hypocenter of the Aketao earthquake, which may restrain the occurrence of the Aketao earthquake (Fig.2c, Fig.3c).However, the

co-seismic and post-seismic stress change of the 1974 Markansu earthquake caused significant stress loading on the rupture zone of the Aketao earthquake. Up to November 2016 before the Aketao earthquake, the stress variation at its hypocenter had reached 0.563MPa. The 2016 Aketao earthquake was significantly accelerated by the Coulomb stress change of historical earthquakes, among which the 1974 earthquake played a major role.

To sum up, all the historical earthquakes in the study area occurred in the zone where the co-seismic and post-seismic Coulomb stress was increased. Before the 1896 Taxkorgan earthquake, the 1974 Markansu earthquake and the 2016 Aketao earthquake, the Coulomb stress variations at their hypocenters were 0.251MPa, 0.013MPa and 0.563MPa, respectively (Fig.3), all exceeding the threshold value of 0.01MPa. It can be concluded that these three earthquakes were triggered by the co-seismic and post-seismic stress change of preceding earthquakes.

4.2 Results stability analysis

4.2.1 Validation of rupture model of the 1974 and 1985 earthquakes

All the historical strong earthquakes discussed in this paper along the KES and adjacent areas since 1895 have a specific slip model except the 1974 Markansu earthquake and the 1985 Ulugqat one. The co-seismic slip models of these two earthquakes are obtained mainly based on the focal mechanism of the main shock and empirical equations [19]. The reliability of empirical slip models needs to be validated. Generally speaking, the co-seismic stress change caused by the main shock can advance the occurrence of most aftershocks. By analyzing the correspondence between the co-seismic Coulomb stress fields and the distribution of aftershocks (Fig.4), we validate the reliability of the empirical slip models of the 1974 Markansu earthquake and the 1895 Ulugqat earthquake.

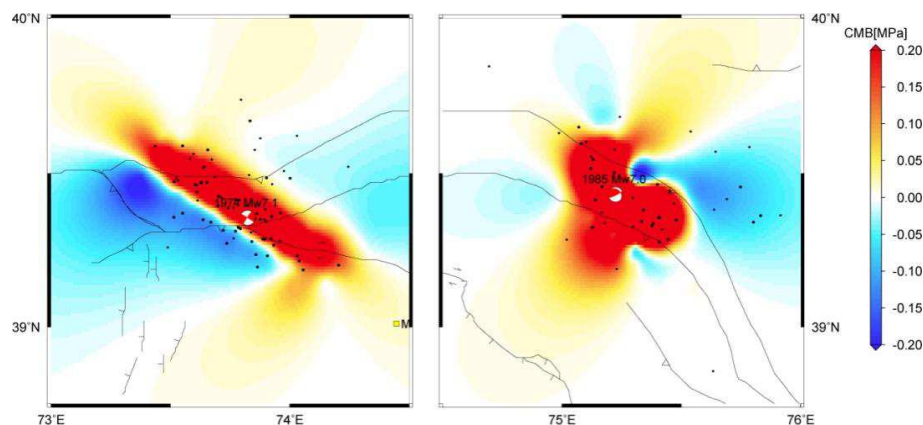


Fig. 4 Co-seismic Coulomb stress fields and aftershock distributions of the 1974 and 1895 earthquakes

Since most aftershocks of the 1974 and 1985 earthquakes do not have a clear focal mechanism, we take regional tectonic stress field into account and calculate the co-seismic Coulomb stress change induced by these two earthquakes by taking the optimal rupture plane as the receiver fault. Considering that the occurrence of a strong earthquake usually shows the tectonic background in this area, we take the focal mechanism of the main shock as the rupture mechanism of the background stress field in our calculation. When the regional tectonic stress field is considered, the absolute stress state in the crust consists of background tectonic stress field and the stress field caused by earthquakes. Based on the absolute stress state of the crust and the Coulomb rupture criterion, the optimal rupture direction in the surrounding area after an earthquake is calculated, and the Coulomb stress change on this optimal rupture plane is then obtained. Our results show that the co-seismic stress fields of the 1974 and 1985 earthquakes are distributed in sectors, and both contain four stress-enhanced zones where most aftershocks are distributed. The correspondence between the co-seismic stress field and the aftershock distribution also proves the reliability of the empirical slip models for the 1974 and 1985 earthquakes.

4.2.2 Effect of parameter value in the calculation

Based on the mathematic model of Coulomb stress, it can be concluded that the calculation of co-seismic Coulomb stress is influenced by the effective friction coefficient, while the post-seismic viscoelastic Coulomb stress is also correlated with the viscosity coefficients of the lower crust and the upper mantle. This section selects different effective friction values and viscosity values to analyze the effect of parameter uncertainty on the ultimate calculation results.

In the mathematic model of Coulomb stress, the calculation of normal stress and shear stress have no relation with the effective friction coefficient, but the change of friction coefficient affects the weight of normal stress change in the Coulomb stress change. When conditions for stress remain constant, the friction coefficient has a linear impact on the calculation of Coulomb stress [28-29]. In this work, the effective friction coefficient takes on the values of 0.2, 0.4 and 0.6 to calculate the stress evolution at the hypocenter of the 2016 Aketao earthquake (Fig.5a). As the value varies, the Coulomb stress at the hypocenter has a linear change with the friction coefficient, but the basic characteristics of the stress evolution show little difference. Hence, the value of effective friction coefficient does not affect the variation tendency of Coulomb stress.

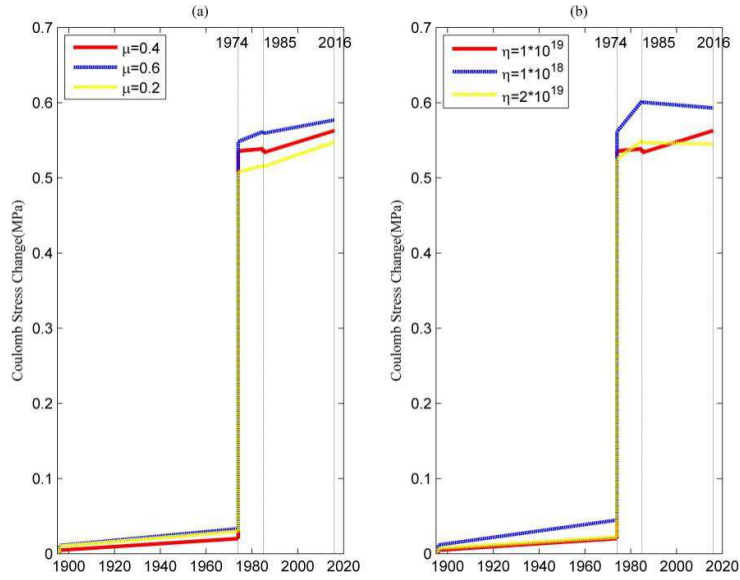


Fig. 5 Effect of different parameter values in the calculation

Based on the three different values of the viscosity coefficient (Table 3), we obtain the stress evolution at the hypocenter of the 2016 Aketao earthquake (Fig.5b). Fig. 5 shows that Model 2 with a lower viscosity value for the lower crust has a higher rate for post-seismic viscoelastic stress release. The uncertainty of the viscosity coefficient mainly affects the post-seismic stress release rate. As the viscosity value changes, the difference of stress variations at the hypocenter of the Aketao earthquake is within 0.1MPa, which means that the uncertainty of viscosity coefficient does not have a significant impact on the final results.

4.3 Stress accumulation along the KES and seismic hazard

In order to probe into the stress accumulation along the KES and the present seismic hazard, we calculate the co-seismic and post-seismic Coulomb stress accumulation caused by historical earthquakes along the KES since 1895, and obtain the stress distribution in the rupture plane at the depth of 0-30 km (Fig.6). Changes of the strike and dip angles of different faults are taken into account, and the variation of viscoelastic Coulomb stress is calculated until November 26, 2016 (just after the Aketao earthquake).

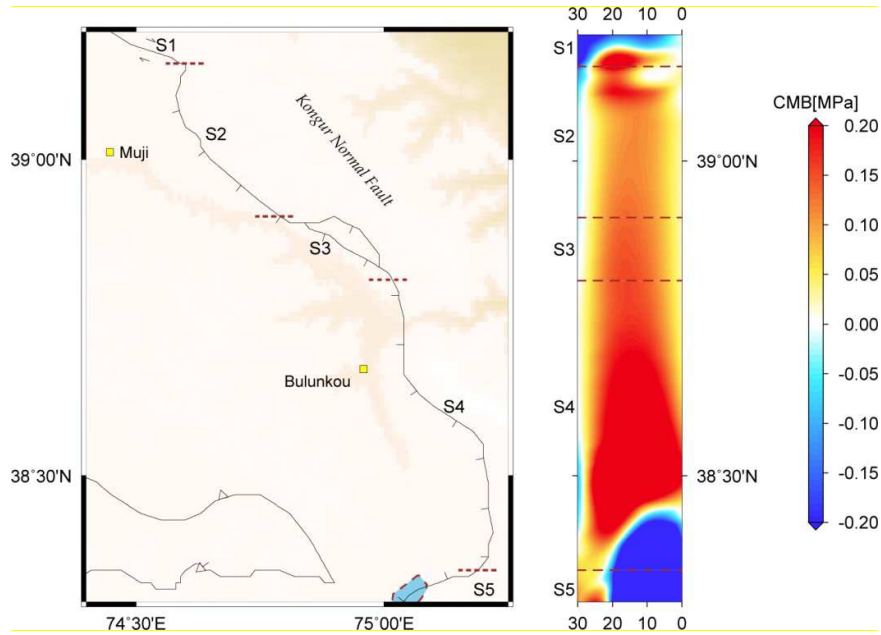


Fig. 6 Stress accumulation along the KES from 1895 to 2016 (co-seismic and post-seismic)

S1: eastern segment of Muji Fault; S2: northern segment of Kungai Fault; S3: southern segment of Kungai Fault;

S4: Kongur Normal Fault; S5: northern segment of MuztagNormal Fault

The 1896 Taxkorgan earthquake caused rupture at the middle segment of the Muztag Ata Fault, and the 2016 Aketao earthquake fractured almost the whole Muji Fault [30]. The co-seismic and post-seismic effects of the above two earthquakes resulted in two stress shadow zones which covered the eastern Muji Fault, northern Muztag Fault and southern Kongur Normal Fault (Fig.6). On the other hand, historical earthquakes increased the stress on most segments of the southern Kungai Fault and Kongur Normal Fault, and formed two high-stress areas at Qimugan segment on the Kungai Fault and Bulunkou segment on the Kongur Fault, where the maximum stress variations were 0.247MPa and 0.587MPa, respectively.

The Qimugan segment of the Kungai Fault is almost vertically intersected with the eastern segment of the Muji Fault (Fig.6), which is prone to stress accumulation[31]. The E-W extension rate of the northern segment of Kungai Fault is about 6.8 mm/a, equal to the dip-slip rate of 7.2 mm/a (Table 1). According to Shen et al.[29], suppose that the tectonic deformation takes place within the range of 100 km and the crust shear modulus is 4×10^{10} Pa, a 7.2 mm/a dip-slip rate at the Qimugan segment can cause 2880 Pa/a stress accumulation. The peak value for stress change at this segment is 0.247 MPa, corresponding to ~86 years tectonic loading.

According to the statistics from GPS survey stations on both sides of the Kongur Normal

Fault near Bulunkou, the current E-W extension rate of this fault is $5.1 \pm 0.8 \text{ mm/a}$ [2], equal to a stress accumulation rate of $1720 \sim 2360 \text{ Pa/a}$. In this way, the peak value of stress variation at Bulunkou segment is 0.587 MPa which corresponds to tectonic loading of 249~341 years. The Kongur Normal Fault is extended in an S-like shape, and stress is prone to be accumulated where the strike of the fault changes. Since no $M_w > 7.0$ earthquakes occurred on the Kongur Fault for hundreds of years, it is likely that the tectonic stress accumulation has reached a high level.

The $M_w 6.6$ Aketao earthquake in 2016 and the $M_w 7.2$ Tajikistan earthquake in 2015 on the Karakul Rift in the middle Pamir are both shallow strike slip earthquakes, which reflects that the current tectonic deformation in the Pamir is mainly E-W extension [2], and the KES plays an important part in the extension process. The Coulomb stress induced by historical earthquakes has increased in a region of 80-km-long segment of the KES, which is equivalent to an $M_w 7.5$ earthquake. The present seismic hazard along the KES is worthy of attention.

5 Discussions and Conclusions

5.1 Interaction among historical earthquakes along the KES

We calculate the co-seismic and post-seismic Coulomb stress change caused by four historical strong earthquakes in the KES and its adjacent areas since 1895. Results show that the co-seismic and post-seismic process of historical earthquakes caused stress loading on the rupture planes of later earthquakes. All of historical earthquakes after 1895 happened in the zones where the co-seismic and post-seismic Coulomb stress was enhanced: prior to the 1896 Taxkorgan earthquake, the 1974 Markansu one and the 2016 Aketao one, stress variations at their hypocenters were 0.251 MPa , 0.013 MPa and 0.563 MPa , respectively, all surpassing the threshold value of 0.01 MPa for stress triggering. Hence, the co-seismic and post-seismic stress change of historical earthquakes promoted the above three earthquakes.

Numerical results suggested that the preceding earthquakes prompt the occurrence of the subsequent ones, and the post-seismic viscoelastic Coulomb stress change plays a key role in the process. For example, during the Coulomb stress evolution at the hypocenter of the 1974 Markansu earthquake, the post-seismic stress variation is even larger than the co-seismic one, which demonstrates that the viscoelastic relaxation effect can significantly change the stress state in the surrounding areas after strong earthquakes. Similar phenomena are also found in the studies

of stress evolutions along the San Andreas Fault, the Longmenshan Fault and the Xianshuihe Fault [12, 32-35].

5.2 Current seismic hazard along the KES

Historical seismic activities caused stress loading on most segments of the Kungai Fault and the Kongur Fault along the KES, and resulted in two high-stress areas at Qimugan segment and Bulunkou segment, where the peak values for stress change corresponds to tectonic loading of ~86 and 249~341 years, respectively. If overall rupture happens along the above two faults, the effect is equivalent to an $M_w7.5$ earthquake.

At present, the major tectonic activities on the northeastern Pamir are dominated by the E-W oriented extensions, among which the KES plays an important role in the internal extension of the Pamir Plateau because it absorbs an extensional amount of 3-11mm/a. The Muztag Fault and Taheman Fault on the southern segment of the KES jointly generated the $M_w7.0$ Taxkorgan earthquakes in 1895 and 1896. The Muji Fault in the north also experienced the $M_w6.6$ Aketao earthquake in 2016. However, the Kungai Fault and the Kongur Fault have not experienced any $M_w>7.0$ earthquakes for hundreds of years, therefore becoming seismic gaps in the northeastern Pamir. Both of these two faults have high stress accumulation and the capability to independently generate $M_w>7.0$ earthquakes. In addition, the Qimugan segment and the Bulunkou segment are located at the faults' turning area where the stress is concentrated with high extensional rate. Therefore, the seismic hazard on these two faults deserves much attention.

5.3 Discussions

After the main shock, aftershocks may also affect the stress state on the surrounding faults, but the focal mechanism and rupture distribution of most aftershocks are not clear. Studies have also shown that the energy released by aftershocks cannot be compared with those caused by the main shock [36], and the stress change caused by aftershocks cannot change the distribution character of the Coulomb stress change. In addition, none of the historical earthquakes involved in this work are recorded to experienced $M_w>6.5$ aftershocks, so the effects of aftershocks are not included. We analyze the characteristics of stress evolution along the KES since 1895, which may serve as a reference for seismic hazard assessment in the study area. However, the earthquake preparation is quite complex, and the earthquake and its magnitude fundamentally depend on the strength of rocks on the rupture plane and whether the stress has reached critical instability state.

Acknowledgements: This study was funded by the Spark Program of Earthquake Technology of CEA (XH17023Y); the National Natural Science Foundation of China (41604079, 41504011, 41574017, 41541029) and the Science and Technology Partnership Program of Shanghai Cooperation Organization (2017E01030). Some figures were completed with Generic Mapping Tools (GMT) (Wessel & Smith, 1995). We also feel grateful for these supports and help.

References :

1. Qiao Xuejun, Wang Qi, Yang Saomin, Li Jie. Study on the focal mechanism and deformation characteristics for the 2008 Mw6.7 Wujia earthquake, Xinjiang by InSAR, Chinese Journal Geophysics 57(6) (2014) 1805-1813.
2. Chen Jie, Li Tao, Li Wenqiao, Yuan Zhaode. Late Cenozoic and present tectonic deformation in the Pamir salient, Northwestern China, Seismology and Geology 33(02) (2011) 241-259.
3. Li Wenqiao, Chen Jie, Yuan Zhaode, Huang Mingda, Li Tao. Coseismic surface ruptures of multi segments and seismogenic fault of the Tashkorgan earthquake in Pamir, 1895, Seismology and Geology, 33(2) (2011) 260-276.
4. Chen Jie, Li Tao, Sun Jianbao, Fang Lihua, Yao Yuan, Li Yuehua, Wang Haoran, Fu Bo. Coseismic surface ruptures and seismogenic Muji fault of the 25 November 2016 Arketao Mw6.6 earthquake in Northern Pamir, Seismology and Geology, (04) (2016) 1160-1174.
5. Metzger S, Schurr B, Schoene T, et al. Rupture model of the 2015 M7.2 Sarez, Central Pamir, earthquake and the importance of strike-slip faulting in the Pamir interior. Abstract T11A-2579 presented at 2011 Fall Meeting, AGU, San Francisco, Calif (2016) 12-16.
6. Xiong Wei, Tan Kai, Liu Gang, Qiao Xuejun, Nie Zhaosheng. Coseismic and postseismic Coulomb stress changes on surrounding major faults caused by the 2015 Nepal Mw7.9 earthquake, Chinese Journal Geophysics, 58(11) (2015) 4305-4316.
7. Stein R S, Barka A A, Dieterich J H. Progressive failure on the North Anatolian fault since 1939 by earthquake stress triggering, Geophys. J. Int., 128 (1997) 594-604.
8. Stein R S. The role of stress transfer in earthquake occurrence. Nature, 402 (1999) 605-609.
9. Stein R S. Earthquake conversations. Sci Am, 288 (2003) 72-79.
10. Parsons, T., Toda, S., Stein, R. S., Barka, A., Dieterich, J. H. Heightened odds of large earthquakes near Istanbul: An interaction-based probability calculation, Science, 288 (2000) 661-665.

11. XiongXiong, Shan Bin, Zheng Yong, Wang Rongjiang. Stress transfer and its implication for earthquake hazard on the Kunlun Fault, Tibet, *Tectonophysics*,482 (2010) 216-225.
12. Shan Bin, XiongXiong, Wang Rongjiang, Zheng Yong, Yang Song. Coulomb stress evolution along Xianshuihe-Xiaojiang Fault System since 1713 and its interaction with Wenchuan earthquake, May 12, 2008. *Earth and Planetary Science letters*, 377-378(2013)199-210.
13. Chevalier ML, Li Haibing, Pan Jiawei, Pei Junling, Wu Fuyao, Xu Wei, Sun Zhiming, Liu Dongliang. Fast slip-rate along the northern end of the Karakorum fault system, western Tibet,*Geophys. Res. Lett.*,38(22)(2011) 116-120.
14. ChenJie, QuGuosheng, Hu Jun, Feng Xianyue. Arcuate thrust tectonics and its contemporary seismicity in the eastern section of the external zone of the Pamir,*Seismology and Geology*,19(4) (1997) 301-312.
15. Jackson J, Molnar P, Patton H, Fitch T. Seismotectonic aspects of the Markansu Valley, Tajikstan, earthquake of August 11, 1974, *J Geophys Res*,84(1979)8157-9187.
16. Yang Maoyuan, Shu Peiyi, Zhou Wenhui. Determination of the source parameters of the Wuqia earthquake in Xinjiang from far field P-Waveform, *Earthquake Research In China*, (04)(1985) 77-82.
17. Feng Xianyue. *The Paleoearthquakes in Xinjiang Region, China*. Xinjiang Science, Technology and HealthPublishing House, Urumchi. (1997)33-34.
18. Burtman V S, Molnar P. Geological and geophysical evidence for deep subduction of continental crust beneath the Pamir, *Special Paper GeolSoc Am*, 281 (1993) 76.
19. Wells D L, Coppersmith K J. New empirical relationships among magnitude, rupture length, rupture width, rupture area, and surface displacement,*Bull.Seismol.Soc.Am*. 84(1994) 974-1002.
20. PapadimitriouE, WenXueze, KarakostasV, JinXueshen. Earthquake triggering along the Xianshuihe Fault zone of western Sichuan, China, *PureAppl.Geophys*.161(2004) 1683–1707.
21. Xiong Wei, Tan Kai, QiaoXuejun, Liu Gang, NieZhaosheng. Coseismic, Postseismic and Interseismic Coulomb Stress Evolution Along the Himalayan Main Frontal Thrust Since 1803. *PureAppl.Geophys*.174 (2017) 1889-1905.
22. Li Jie, Liu Gang, QiaoXuejun, Xiong Wei, Wang Qi. Rupture characteristics of the 25 November 2016 Akteo earthquake (Mw6.6) in eastern Pamir revealed by GPS and teleseismic data, *PureAppl.Geophys*.175(2)(2018)1-13.
23. Scholz, C.H. *The Mechanics of Earthquakes and Faulting*. Cambridge Univ. Press, New York. (1990)p.439.

24. Parsons T, Stein R S, Simpson R W. Stress sensitivity of fault seismicity: a comparison between limited-offset oblique and major strike-slip faults, *J Geophys Res.*, 104(1999)20183-20202.
25. Wang Rongjiang, Lorenzo-Martin F, Roth F. PSGRN/PSCMP—a new code for calculating co- and post-seismic deformation, geoid and gravity changes based on the viscoelastic-gravitational dislocation theory. *Comput.Geosci.* 32(4) (2006) 527–541.
26. Shi Yaolin, Cao Jianlin. Lithosphere effective viscosity of continental China. *Earth Sci. Front.* 15(3) (2008) 82–95.
27. Wen Yangmao, Li Zhenghong, Xu Caijun, Isabelle Ryder, Roland Burgmann. Postseismic motion after the 2001 Mw 7.8 Koxili earthquake in Tibet observed by InSAR time series. *J. Geophys. Res.* 117(8)(2012) B08405.
28. Xu Caijun, Wang Jianjun, Li Zhenghong, et al. Applying the Coulomb failure function with an optimally oriented plane to the 2008 Mw 7.9 Wenchuan earthquake triggering, *Tectonophysics*, 491(1-4) (2010) 119-126.
29. Shan Bin, Li Jiahang, Han Libo, Fang Lihua, Yang Song, Jin Bikai, Zheng Yong, Xiong Xiong. Coseismic Coulomb stress change caused by 2010 MS=7.1 Yushu earthquake and its influence to 2011 MS=5.2 Nangqên earthquake, *Chinese Journal Geophysics*, 55(09) (2012) 3028-3042.
30. Wang Shuai, Xu Caijun, Wen Yangmao, Yin Zhi, Jiang Guoyan, Fang Lihua. Slip Model for the 25 November 2016 Mw 6.6 Ake Tao Earthquake, Western China, Revealed by Sentinel-1 and ALOS-2 Observations. *Remote Sens.* 9(9) (2017) doi:10.3390/rs9040325
31. Xu Xiwei, Jiang Guoyan, Yu Guihua. Discussion on seismogenic fault of the Ludian Ms 6.5 earthquake and its tectonic attribution. *Chinese Journal Geophysics*, 57(9) (2014) 3060-3068.
32. Freed A M, Lin Jian. Delayed triggering of the 1999 Hector Mine earthquake by viscoelastic stress transfer. *Nature*, 411(6834) (2001) 180–183.
33. Freed A M, Ali S T, Burgmann R. Evolution of stress in Southern California for the past 200 years from coseismic, postseismic and interseismic stress changes. *Geophys.J.Int.*, 169(3)(2007) 1164–1179.
34. Ali S T, Freed A M, Calais E. Coulomb stress evolution in Northeastern Caribbean over the past 250 years due to coseismic, postseismic and interseismic deformation. *Geophys.J.Int.*, 174 (2008) 904–918.
35. Lei Xinglin, Ma Shengli, Su Jinrong, Wang Xiaolong. Inelastic triggering of the 2013 Mw 6.6 Lushan earthquake by the 2008 Mw 7.9 Wenchuan earthquake, *Seismology and Geology*, 35(2)(2013) 411-422.
36. Wan Yongge, Shen Zhengkang, Sheng Shuzhong, Xu Xiaofeng. The influence of 2008 Wenchuan earthquake on surrounding faults. *Acta Seismologica Sinica*, 31(2) (2009) 128-139.